ID: 2016-ISFT-121

The Evaluation of Energy Consumption for Thermal Type Seawater Desalination between MED-MVC and Conventional MSF

Hanshik Chung[1], Hyomin Jeong[2], Soon-Ho Choi[3], Seung Gue Park[4]

[1,2,3]Department of Energy and Mechanical Engineering, Gyeongsang National University, 445, Inpyeong-Dong, Tongyeong 650-160, Gyeongsang Namdo, Korea
[2]Offshore Commissioning Team, Dawoo Ship Marine Engineering Co. Ltd, Korea
[1]hschung@gnu.ac.kr

Abstract: *Seawater desalination is classified as thermal type and membrane type. Although the membrane type, which is usually reverse osmosis (RO), which will be main in future desalination market due to its simplicity and operational economy, the thermal type is still dominant in large scale seawater desalination plants. In the case of the thermal type desalination, it is known that the multi-effect desalination with a mechanical vapor compressor (MED-MVC) is best economical. In this study, the energy consumption for the thermal type seawater desalination is compared between MED-TVC and the conventional multi-stage flashing type (MSF), the latter of which is the main of a large scale plant. For the evaluation of the required energy to product fresh water, the MED-TVC is based on the CFD simulation result for the MED-TVC and the MSF is based on the theoretical calculation. The CFD simulation for the MED-TVC system was analyzed by using a Reynolds-Averaged Navier Stokes equation with an SST $\kappa-\omega$ turbulence model using a frozen rotor interface. The best and the worst operational cases of the MED-TVC were compared with the MSF type under the assumptions of the same operating conditions. The results of this study indicates that the MED-MVC type is best efficient in the thermal type seawater desalination and provides the operational ranges of the centrifugal type vapor compressor, which will be guidelines for designing it.*

Keywords: *CFD simulation, seawater desalination, multi effect distillation, mechanical vapor compressor, multi-stage flashing*

1. INTRODUCTION

The enrichment of liquid has performed through membrane type or thermal type processes; the former is usually adopted in desalination and the latter in polluted water treatment, liquid food concentration or chemical distillation.

Although the membrane type is dominant in recent seawater desalination market to a capacity of 5000 ton/day, the thermal type is still effective in a large scale capacity plants over it. The thermal type seawater desalination process is classified into multi-stage flashing (MSF) distillation and multi-effect distillation (MED).

The MED process recompresses the evaporated vapour form seawater and reutilizes it to heat seawater while the MSF type simply evaporates seawater through the multi-stages. Therefore, the MED type is more economic than the MSF type from the viewpoint of operating cost. In the MED type, the evaporated vapour is recompressed through the thermal vapour compressor (TVC) or the mechanical vapour compressor (MVC); the former is called the MED-TVC type and the latter is called the MED-MVC type. At present, the commercial experiences of the MED type is up to 70,000~80,000 ton/day capacity in the MED-TVC and under 10,000 ton/day capacity in the MED-MVC type [1,2] while the MSF type has many experiences in the capacities over 100,000 ton/day.

In the Middle East region, the existing desalination plants are almost the MSF type because the water shortage is serious and, therefore, a large scale is required as possible; the desalination plant is constructed together with the power plant and, therefore, the steam required for desalination can be easily supplied from it. The steam to be used as a heating source for the MSF process is extracted from the low-pressure steam turbine and the temperature of an extracted steam is usually in the range from 110~120 ^{o}C, which is called top brine temperature (TBT). In the contrast with the MSF type, the TBT of the MED type is usually about 70 ^{o}C due to its evaporating characteristics.

In this study, the authors performed the theoretical study to compare the required energy for unit fresh water production of the MSF and MED-MVC, which will provide the design criteria to the engineers related with the seawater desalination process. For evaluating the performance of the MED-MVC, the CFD simulation for the MED-TVC system was performed by using a Reynolds-Averaged Navier

Stokes equation with an SST □□□ turbulence model using a frozen rotor interface.

2. THE SEAWATER DESALINATION SYSTEM

2.1 MSF DESALINATION

The process of the thermal type seawater desalination is basically to evaporate seawater; the evaporated vapor from seawater is condensed on the surfaces of the cooling tubes, which are installed in the upper section of the evaporators as shown in Fig. 1 (a); the evaporated steam is condensed on the outside surface on the tubes, in which the cooling seawater is flowing; the condensed fresh water is supplied to the utilities after post-treatment, which are usually sterilization and re-hardening. The purity of produced fresh water from the thermal type can maintain less than 10 ppm salinity because the evaporated steam from seawater is pure water while the RO membrane type is about 200~400 ppm. The MSF type desalination plants have been introduced and operated commercially from 1970s and this type is already a considerable market share in the Middle East [3,4].

The basic configuration of the OT-MSF type desalination plant is shown in Fig. 1. The seawater is supplied to the last evaporating chamber by the seawater supply pump and flows into the cooling tube banks installed on the top section of the evaporating chambers; after passing the cooling tube bank, the cooling seawater is supplied to the next evaporator's cooling tube bank and so on; this cooling water condenses the evaporated steam in the brine pool and the steam is converted to the fresh water; the produced fresh water in each stage is collected in the condensate tray and discharged out in the cascade way.

The cooling seawater passing through the tube banks of each stage is discharged from the first stage and its temperature has already increased because it absorbed the latent heat of the evaporated steam in each stage. The cooling seawater discharged from the first stage is heated over the operating temperature of the first stage by the brine heater as shown in the left side of Fig. 1; the heating source of the brine heater is the steam extracted from the low pressure turbine of a power plant.

The heated seawater in the brine heater is supplied into the brine pool of the first stage and the supplied seawater is evaporated because its temperature is higher than the saturated temperature corresponding to the operating pressure of the first stage. The evaporated steam passes through the demister, which performs the role of screening the seawater liquid droplets. Since the flashing evaporation is occurred violently on the surface of the brine pool, a number of tiny seawater droplets even micro-sized are sufficiently floated in the evaporator space. The demister, which is the fine metallic meshes stacked in a number of layers, prevents the entrainment of such tiny seawater droplets and therefore maintains the purity of the condensed fresh water to a required salinity.

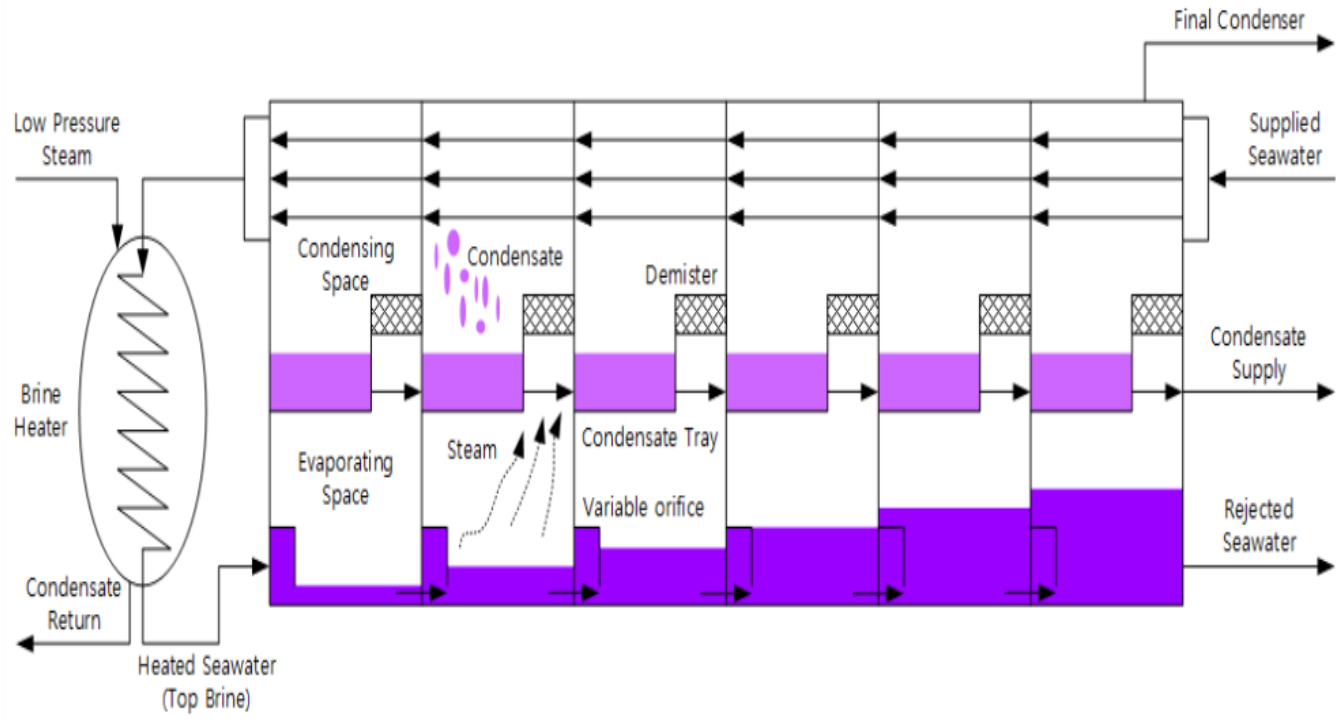

Fig. 1. Schematic diagram of the OT-MSF seawater desalination system.
This figure was cited from the reference [5] under the author's permission.

2.2 MED-MVC DESALINATION

The mechanical vapor compression (MVC) desalination process is generally used in combination with other processes and by itself for small and medium scale seawater desalting applications. The heat for evaporating the water comes from the compression of vapor rather than the direct el

The plants that use this process are also designed to take advantage of the principle of reducing the boiling point temperature by decreasing the operating pressure. Steam ejectors (thermal vapor compression) and mechanical vapor compressors (MVC) are used in the compression cycle to run the process. The mechanical compressor is usually electrically or diesel driven, allowing the sole use of electrical or mechanical energy to produce water by distillation.

The MVC units have been built in a variety of configurations to promote the exchange of heat to evaporate the seawater. Fig. 2 illustrates a simplified method in which a mechanical compressor is used to generate the heat for evaporation. All steam is removed by a mechanical compressor from the last effect and introduced as heating steam into the first effect after compression where it condenses on the cold side of the heat transfer surface.

Seawater is sprayed, or otherwise distributed on the other vapor compression desalination is a distillation process where the evaporation of sea or saline water is obtained by the application of heat delivered by compressed vapor.

One of the main features of a detailed MVC model is the model for the power consumption of the vapor compressor, which is developed as a function of the compressor efficiency and isentropic power, as well as the actual and ideal isentropic vapor temperatures. An important parameter for increasing the MVC capacity is developing a higher volumetric flow and head or pressure ratio. A higher head makes it possible to effectively utilize the MED-MVC [6].

In addition, the most desirable compressor is one that is able to operate at the highest mass flow rate and highest possible discharge pressure. One requirement for turbomachinery is an extended operation range because of the sensitivity of transient operation on the compressor surge margin [7]. The extension of the operation range and continuous improvements in the stage performance have been achieved through a better understanding of the flow physics such as secondary flow field development [8]. The accurate prediction of the MVC performance is needed to promote the reliability of the process. Flow visualization methods are useful to determine the different flow patterns at each operating condition [9]. Even some additional improvements are still possible through a better understanding of the flow behavior over the entire operational range. Currently, centrifugal compressors are designed for optimal operation at a single speed based on the design speed. The design speed is usually set at the point where the compressor will operate for the longest duration. However, compressors must also operate at speeds other than the design point for various amounts of time [10]. A low efficiency at these off-design points can lead to problematic engine starts and poor performance during acceleration. Furthermore, as the compressor becomes more optimized for the design speed, it is increasingly likely that this effort can adversely affect its performance at off-design conditions [11].

In this paper, a compressor model is used for a multistage centrifugal compressor that will be implemented in an MED-MVC desalination system. The compressor is designed without a twist angle for the impeller blade at each stage out of consideration for a low manufacturing cost. Based on the blade shape, this centrifugal compressor is a backswept type.

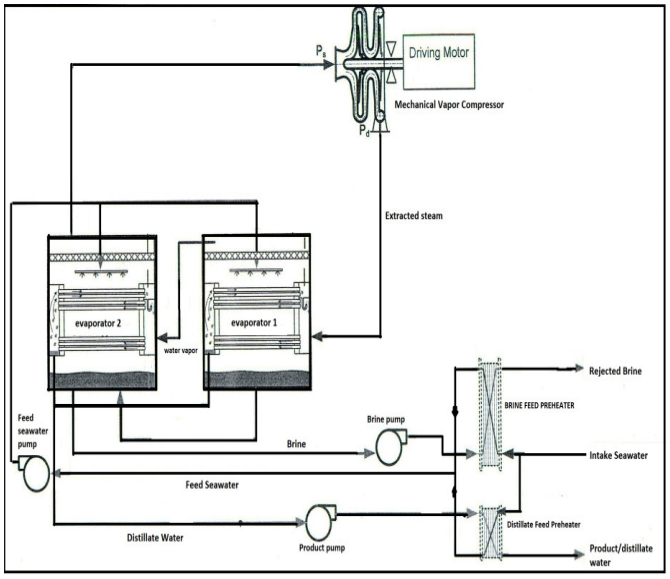

Fig. 2. Schematic diagram of MED-MVC desalination

3. RESULTS OF CALCULATION AND CFD SIMULLATION

3.1 MSF DESALINATION

The whole heat energy consumed in the MSF system is the low pressure steam, which is supplied to the brine heater and the steam ejector. The former is to evaporate seawater and the latter is to operate the vacuum system. Since the steam flowrate required for the steam ejector will be varied with the plant capacities and the makers' intrinsic designs, it is not considered in this study. Therefore the pump powers for the transportation of seawater and fresh water are considered including the heat energy for the brine heater.

The evaporated quantities of each stage can be calculated as follows;

$$m_{eva1} = \frac{m_1 \cdot c_{p1}\left(T_{TBT} - T_{s1}\right)}{h_{fg1}}, \quad (1)$$

$$m_2 = m_1 - m_{eva2}, \quad (2)$$

$$m_{eva2} = \frac{m_2 \cdot c_{p2}\left(T_{s1} - T_{s2}\right)}{h_{fg2}}, \quad (3)$$

$$m_N = m_{N-1} - m_{evaN-1} \quad (4)$$

$$m_{evaN} = \frac{m_N \cdot c_{pN}\left(T_{sN-1} - T_{sN}\right)}{h_{fgN}}. \quad (5)$$

In the above equations, m_N is the brine quantity supplied to the N stage, which is the rested brine after evaporating in the N-1 stage; m_{evaN} is the evaporated quantity in the N stage; T_{sN} is the operating pressure of the N stage, which is the saturated temperature corresponding to the N stage's operating pressure; c_{pN} is the specific heat of the brine supplied to the N stage and h_{fgN} is the latent heat, that is the enthalpy for phase change, in the N stage. These two values are the properties of fluid and will be varied with the pressure and the temperature of each stage.

Table 1 is the summarized calculation results when the variations of the TBTs were applied to an assumed existing plant. It should be noticed that, in the table, the unit of thermal energy is MW and the electrical energy is kW. The calculated values are well consistent with the existing research results [12,13]. From Table 1, the energy consumed to make the unit mass of fresh water is clearly reduced with increasing the TBT and this means that the operating cost can be saved for producing fresh water although the total required energy is increased.

TABLE 1: Calculation results by the variation of the TBTs

	TBT=90	TBT=100	TBT=110	TBT=120
□T_{eva} (1)	.5	3.0	3.5	4.0
M_{fw} (2)	6169.0	7607.0	9042.0	10475.0
T_{cw} (3)	76.02	85.01	93.86	102.56
E_{he} (4)	1592.5	1708.6	1842.1	1992.9
P_{sw} (5)	1636.8	1636.8	1636.8	1636.8
P_{fw} (6)	471.4	581.3	690.9	800.4
P_{br} (7)	731.3	720.1	708.9	697.8
E_{tot} (8)	1595.4	1711.5	1845.1	1966.0
E_{unit} (9)	0.259	0.225	0.204	0.191

Note (1) Temperature difference between the evaporators (^oC)

Note (2) Production of fresh water (kg/hr)

Note (3) Temperature of cooling seawater from the first stage (^oC)

Note (4) Heating energy for brine heater (MW)

Note (5) Power of seawater supply pump (kW)

Note (6) Power of condensate pump (kW)

Note (7) Power of brine rejection pump (kW)

Note (8) Total energy for fresh water (kW)

Note (9) Required energy to produce the unit mass of fresh water (MW/kg)

3.2 MED-MVC DESALINATION

The compressor was modeled as 3D periodic model in a commercial CFD software package (CFX 12). Three sections were used for the multistage centrifugal compressor simulation. To reduce the computational cost, only single passage on each stage was considered as a part of the computational domain .The simulation was modeled as a steady state problem using frozen rotor interface.

The grid structure was tetrahedral unstructured, as shown in Fig. 3. The grid was made 119,291 nodes and 613,893 elements. The grid density was concentrated at the critical areas where the significant phenomena were expected.

The inlet boundary condition was defined as a subsonic inlet, and the temperature and total pressure were measured. The turbulence intensity was defined to be about 5%. Periodic boundary conditions were applied to the impeller periodic plane at the middle of the impeller passage. The blade hub and shroud were defined as adiabatic walls.

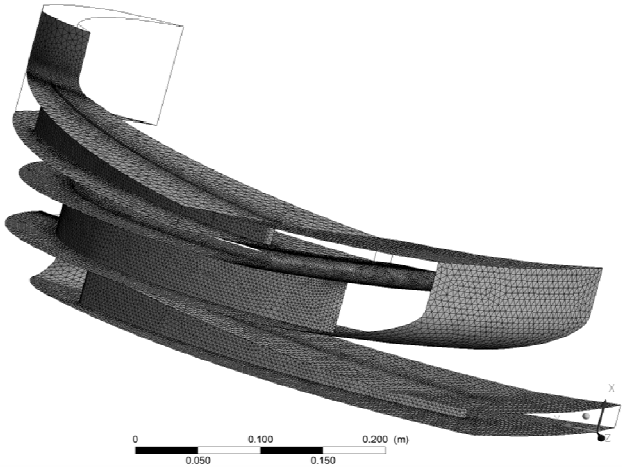

Fig. 3. Grid computational domain

The 3-D Reynolds averaged compressible Navier-Stokes equations together with an SST □□□ turbulence model were solved using a commercial CFD package, CFX 12. The mass and momentum conservation equations are given as follows. □ represents the density (kg/m3), *u* is the

velocity (m/s), p is the pressure (Pa), k is the turbulence kinetic energy (m^2/s^2), μ is the laminar viscosity (kg/m s), and π_t is the turbulence viscosity (kg/m s). The subscripts i, j, and l represent the directions (x,y,z). δ_{ij} is the kronecker delta; it is equal to one when $i = j$, otherwise it is zero [14].

$$\frac{\partial}{\partial x_i}(\rho u_i) = 0 \tag{6}$$

$$\frac{\partial}{\partial x_i}(\rho u_i u_j) = -\frac{\partial p}{\partial x_i} + \frac{\partial p}{\partial x_j}\left[\mu\left(\frac{\partial u_i}{\partial x_j} + \frac{\partial u_j}{\partial x_i} - \frac{2}{3}\delta_{ij}\frac{\partial u_l}{\partial x_l}\right)\right] + \frac{\partial}{\partial x_j}\left[\mu_t\left(\frac{\partial u_i}{\partial x_j} + \frac{\partial u_j}{\partial x_i}\right) - \frac{2}{3}\left(\rho k + \mu_t\frac{\partial u_l}{\partial x_l}\right)\delta_{ij}\right] \tag{7}$$

The shear-stress transport (SST) model is a non-algebraic two-equation turbulence model suggested by Menter as a combination of the $k-\omega$ model and $k-\varepsilon$ model. To take advantage of both, Menter applied the Wilcox $k-\omega$ model in the near wall region and gradually changed it into the standard $k-\varepsilon$ model in the outer wake region. This model is considered one of the best two-equation RANS models and is particularly suitable for a flow separation scenario such as cavity flow [15].

$$\frac{\partial}{\partial t}(\rho k) + \frac{\partial}{\partial x_j}(\rho U_j k) = \tau_{ij}\frac{\partial u_i}{\partial x_j} - \beta^*\rho\omega k + \frac{\partial}{\partial x_j}\left[(\mu + \sigma_k\mu_t)\frac{\partial k}{\partial x_j}\right] \tag{8}$$

$$\frac{\partial}{\partial t}(\rho\omega) + \frac{\partial}{\partial x_j}(\rho U_j\omega) = \tau_{ij}\frac{\gamma}{\nu_t}\frac{\partial u_i}{\partial x_j} - \beta\rho\omega^2 + \frac{\partial}{\partial x_j}\left[(\mu + \sigma_\omega\mu_t)\frac{\partial\omega}{\partial x_j}\right] + 2\rho(1-F_1)\sigma_\omega\frac{1}{\omega}\frac{\partial k}{\partial x_j}\frac{\partial\omega}{\partial x_j} \tag{9}$$

The turbulent shear stress is defined based on Bradshaw's assumption that the shear stress is proportional to the turbulent kinetic energy, k, in the boundary layer, $\tau = \rho a_1 k$, where a_1 is a constant.

The eddy-viscosity is given by

$$\nu_t = \frac{a_1 k}{\max(a_1\omega; \Omega F_1)}, \tag{10}$$

in which Ω is the absolute value of the vortices and F_1 is given by

$$F_1 = \tanh\left[\max^2\left(2\frac{\sqrt{k}}{0.09\omega y}; \frac{500\nu}{y^2\omega}\right)\right]. \tag{11}$$

For the steady state cases, a constant total pressure and total temperature distribution was applied at the inlet of the domain. The fluid properties were set as shown in table 2. An assumption of temperature dependence was made for the fluid property characteristics. Fig. 4 shows the compressor performance map.

Because the compressor model was simulated only at low rotational speeds, only the surge phenomenon can be described by this graph. From this graph, the surge term indicates an instability phenomenon, which occurs at a low flow value. Because of the low flow value, the stage pressure ratio or head does not vary in a stable manner with the flow rate. For a higher rotational speed, the surge margin was narrower than at a lower rotational speed for a low mass flow rate. As seen in fig. 4, it was very dangerous to operate the compressor at a higher rotational speed at a low mass flow rate. Surge from the incidence angle of the fluid flow (stall) was generally caused by important separation phenomena. Surge is characterized by intense and rapid flow and pressure fluctuation throughout the system. Fig. 4 shows that surge occurred when it had a positive slope. This phenomenon was generally accompanied by loud noise and violent vibrations.

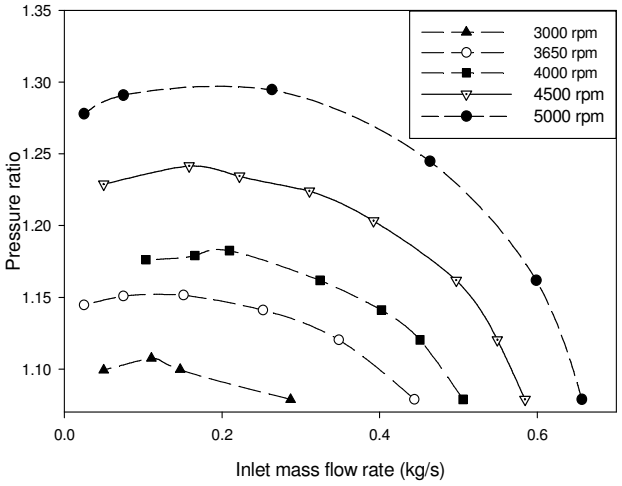

Fig. 4. Compressors performance map at various rotational speeds

4. CONCLUSIONS

The heat input of the MED-MVC was calculated by the law of ideal gas and the mass flowrate of vapor to the compressor, which is the in temperature increase of the vapor due to the compression. In the high pressure ratio of compression, the compressibility factor should be considered. However, in the MED-MVC system, the compressibility effect can be ignored since the vapor supplied to the compressor is very low pressure that is vacuum state. In addition to it, in this study, the compression ratio is only from 1.10 to 1.30, this assumption is reasonable.

The temperature increase by vapor compression was about 2~5 ^oC in this study, which is controlled by the rotational speed of blades, that is rpm. If the rpm of the compressor is increased to the order of 10000, the higher heating temperature of vapor, which means the discharge temperature of vapor, will be obtained.

In this study, the maximum rpm was selected upto 5000 because the motor driven compressor was assumed to be the

two stages. To reach over 10000 rpm, the compressor driver should be changed such as turbine. Nevertheless, the MED-MVC desalination system showed the high efficiency more than 20 % compared with the conventional MSF type.

However, it should be noticed that the MED-MVC type is for small capacity and the MSF type is for large capacity. Since this study was compared only the required energy for producing a unit fresh water, a more in-depth evaluation is needed in order to take into account the economies of scale.

ACKNOWLEDGEMENT

This research was supported by Basic Science Research Program through the National Research Foundation of Korea (NRF) funded by the Ministry of Education (No. 2015R1D1A1A01058030).

REFERENCES

[1] Ophir, A. Gendel, A. Steam driven large multi effect MVC (SD MVC) desalination process for lower energy consumption and desalination costs, Desalination 2007, 205 (1-3), 224-230.

[2] Choi, D. Y.; Kim, C. B.; Song, S. Y.; Choi, S.-H. et al. A Study on the MED-TVC Operating Performance Characteristics of Using the Thermo-Compressor-I (in Korean), Journal of the Korean Society of Marine Engineering 2008, 32 (8), 1185-1191.

[3] Naira, M.; Kumarb, D. Water desalination and challenges: The Middle East perspective: A Review, Desalination and Water Treatment 2013, 51 (10-12), 2030-2040.

[4] Lattemann, S. Development of an Environmental Impact Assessment and Decision Support System for Seawater Desalination Plants 2010, Ph. D Dissertation, Delft University.

[5] Song, C.S. A study on the required energy of a thermal type desalination plant (in Korean), Journal of the Korean Society of Marine Engineering 2014, 38 (9), 1094-1100.

[6] Ettouney, H.M.; El Dessouky, H.T.; Al-Roumi, Y. Analysis of Mechanical Vapor Compression Desalination Process 1998, Kuwait.

[7] Hildebrandt, A.; Genrup, M. Numerical Investigation of the Effect of Different Back Sweep Angle and Exducer Width on the Impeller Outlet Flow Pattern of a Centrifugal Compressor with Vaneless Diffuser, Journal of Turbomachinery ASME 2007, 129, 421-433.

[8] Brun, K. Analysis of Secondary Flow in Centrifugal Impellers, South West Research Institute 2003, San Antonio, TX, Solar Turbine Inc.

[9] Dean, R. On the Unresolved Fluid Dynamics of the Centrifugal Compressor, Advanced Centrifugal Compressors 1971, ASME publications.

[10] Wallis, C.V.; Moussa, Z.M.; Srivasta, B.N. A stage calculation in centrifugal compressor 2002, ICAS 2002 Congress.

[11] Ibaraki, S.; Matsuo, T.; Kuma, H.; Sumida, K.; Suita, T. Aerodynamics of a Transonic Centrifugal Compressor Impeller, Transactions of the ASME J. Turbomachinery 2003, 125, 346-351.

[12] UNESCWA, Role of Desalination in Addressing Water Scarcity, ESCWA Water Development Report 3 2009, Annex I.

[13] UNESCO Center for Membrane Science and Technology, University of New South Wales, Emerging Trends in Desalination: A Review, Waterlines Report Series 2008, 9.

[14] Jiao, K.; Sun, H. Numerical simulation of air flow through turbocharger compressors with dual volute design, Applied Energy Journal 2009, 86 (11), 2494-2506.

[15] Zhisong, L.; Hamed, A. Numerical Simulation of sidewall effects on the acoustic field in transonic cavity, 45th AIAA Aerospace Sciences Meeting and Exhibit 2007, Reno, Nevada, 1456.